Abali *et al. Mechanics of Advanced Materials and Modern Processes* (2015) 1:4
DOI 10.1186/s40759-015-0004-3

Mechanics of Advanced Materials and Modern Processes
a SpringerOpen Journal

RESEARCH ARTICLE Open Access

Strain gradient elasticity with geometric nonlinearities and its computational evaluation

B Emek Abali[1*], Wolfgang H Müller[1] and Victor A Eremeyev[2]

Abstract

Background: The theory of linear elasticity is insufficient at small length scales, e.g., when dealing with micro-devices. In particular, it cannot predict the "size effect" observed at the micro- and nanometer scales. In order to design at such small scales an improvement of the theory of elasticity is necessary, which is referred to as *strain gradient elasticity*.

Methods: There are various approaches in literature, especially for small deformations. In order to include *geometric nonlinearities* we start by discussing the necessary balance equations. Then we present a generic approach for obtaining adequate constitutive equations. By combining balance equations and constitutive relations nonlinear field equations result. We apply a variational formulation to the nonlinear field equations in order to find a *weak* form, which can be solved numerically by using open-source codes.

Results: By using balances of linear and angular momentum we obtain the so-called stress and couple stress as tensors of rank two and three, respectively. Since dealing with tensors an adequate representation theorem can be applied. We propose for an isotropic material a stress with two and a couple stress with three material parameters. For understanding their impact during deformation the numerical solution procedure is performed. By successfully simulating the size effect known from experiments, we verify the proposed theory and its numerical implementation.

Conclusion: Based on representation theorems a self consistent strain gradient theory is presented, discussed, and implemented into a *computational reality*.

Keywords: Size effect, Micromechanics, Constitutive equations

Background

Traditional constitutive models relating stresses and strains are independent of the size and shape of the continuous body. For example, we model the linear response at small deformations with HOOKE's law, which has the same form for huge and small structures. Unfortunately, such a simple approach becomes inadequate at the micrometer scale. One of the basic approaches in statics, the so-called EULER-BERNOULLI beam theory, results in inaccurate solutions at very small dimensions. For example, sub-micrometer structures frequently show a stiffer response than predicted by traditional theory. This so-called *size effect* has been known experimentally for a long time, see, e.g., (Morrison et al. 1939). Formally, the size effect can be modeled by material properties that depend on specimen size. However, in order to include the size effect in a more rational manner, we will generalize the theory of elasticity by means of higher gradient terms. In fact, theories of higher gradients were proposed more than four decades before, cf., (Mindlin and Tiersten 1962; Mindlin and Eshel 1968). They are still under discussion. Moreover, various variants were developed over the last decades, see for an overview (Gurtin et al. (2010), §90). Especially in micromechanics an applicable theory of generalized theory of elasticity becomes necessary, as pointed out by (McFarland and Colton 2005).

We shall discuss deformation and its description in terms of higher gradients of displacement within the framework of continuum mechanics principles. First, we present the balance equations of linear momentum and

*Correspondence: abali@tu-berlin.de
[1]Technische Universität Berlin, Institute of Mechanics, Einsteinufer 5, D10587 Berlin, Germany
Full list of author information is available at the end of the article

angular momentum, and identify their flux terms as stress and couple stress, respectively. Second, when deriving constitutive equations for the stress and the couple stress we use tensorial relations. Balance equations in combination with constitutive equations will result in nonlinear field equations. Third, in order to solve these field equations we generate a *weak* form by using a variational formulation. For the weak form discretization in time is performed by making use of the *finite difference method*. For discretization in space the *finite element method* is used. Fourth, we implement a code in Python, see (Jones et al. 2001), by using a novel collection of open-source packages distributed under the FEniCS project, see (Logg et al. 2011). We publish the code in (Abali 2015) under GNU Public license as stated in (Gnu Public 2007) in order to encourage further studies.

Methods

Governing equations

We apply the standard nomenclature of continuum mechanics including the summation convention on repeated indices and use the initial positions of particles, $\boldsymbol{X}$, as reference frame where all functions are evaluated. Consider a continuum body deforming from its *known* initial frame, $\mathcal{B}_0$, to an *unknown* current frame, $\mathcal{B}$, in time, t. All particles move from their initial positions, $\boldsymbol{X}$, to the current positions, $\boldsymbol{x} = \boldsymbol{x}(\boldsymbol{X}, t)$. We apply Cartesian coordinates and choose two particles 1 and 2 with current positions:

$$\overset{1}{x}_i = x_i(\overset{1}{X}_j, t)\,, \quad \overset{2}{x}_i = x_i(\overset{2}{X}_j, t)\,, \quad i,j = 1,2,3\,. \tag{1}$$

The distance between these particles reads

$$\Delta x = \sqrt{\Delta x_i \Delta x_i}\,, \quad \Delta x_i = \overset{1}{x}_i - \overset{2}{x}_i\,. \tag{2}$$

The current distance vector, Δx_i, can be expressed by expanding the position of one particle about the position of the other particle by using a TAYLOR series:

$$\begin{aligned}
\overset{1}{x}_i &= x_i\left(\overset{1}{\boldsymbol{X}}, t\right) = x_i\left(\overset{2}{\boldsymbol{X}}, t\right) + \frac{\partial^2 x_i}{\partial X_j}\Big|_{\overset{2}{\boldsymbol{X}},t}\left(\overset{1}{X}_j - \overset{2}{X}_j\right) + \\
&+ \frac{1}{2}\frac{\partial^2 x_i}{\partial X_j \partial X_k}\Big|_{\overset{2}{\boldsymbol{X}},t}\left(\overset{1}{X}_j - \overset{2}{X}_j\right)\left(\overset{1}{X}_k - \overset{2}{X}_k\right) + \mathcal{O}\left(\left(\overset{1}{\boldsymbol{X}} - \overset{2}{\boldsymbol{X}}\right)^3\right)\,, \\
\overset{1}{x}_i - \overset{2}{x}_i &= \Delta x_i = \frac{\partial x_i}{\partial X_j}\Delta X_j + \frac{1}{2}\frac{\partial^2 x_i}{\partial X_j \partial X_k}\Delta X_j \Delta X_k + \mathcal{O}(\Delta \boldsymbol{X}^3)\,,
\end{aligned} \tag{3}$$

with $\Delta \overset{1}{X}_i = \overset{1}{X}_i - \overset{2}{X}_i$. If the initial and current distances become infinitesimal, $\Delta X_i \to \mathrm{d}X_i$ and $\Delta x_i \to \mathrm{d}x_i$, respectively, we obtain the transformation property for the line element by neglecting second order terms:

$$\mathrm{d}x_i = F_{ij}\,\mathrm{d}X_j\,, \quad F_{ij} = \frac{\partial x_i}{\partial X_j}\,, \tag{4}$$

where the deformation gradient, F_{ij}, has been introduced as transformation between the line elements (distances) in the initial and current frames. This transformation leads to the transformation of the current surface element, $\mathrm{d}a_i$, and volume element, $\mathrm{d}v$, onto the initial surface element, $\mathrm{d}A_i$, and volume element, $\mathrm{d}V$, such that:

$$\mathrm{d}a_i = (\boldsymbol{F}^{-1})_{ki} J \mathrm{d}A_k\,, \quad \mathrm{d}v = J\mathrm{d}V\,, \quad J = \det(\boldsymbol{F})\,. \tag{5}$$

In *local* continuum mechanics it is assumed that the particles interact within the local neighborhood, where the distance becomes infinitesimal such that the first gradient describes the behavior of material accurately. We can generalize the behavior by including the second gradient, which enables an interaction of particles in a greater neighborhood. This theory is *nonlocal* and we need different equations restricting the first and the second gradients.

The formulation is easier to develop in displacements, $u_i = x_i - X_i$, we introduce

$$u_{i,j} = \frac{\partial x_i}{\partial X_j} - \delta_{ij}\,, \quad u_{i,jk} = \frac{\partial^2 x_i}{\partial X_j \partial X_k}\,. \tag{6}$$

The quantities $u_{i,j}$ and $u_{i,jk}$ are independent locally, because we cannot determine the derivative of a function at a point just by knowing its value at that point. Since these two quantities are independent, we need two governing equations. We propose to apply two balance equations of momenta in the current frame:

$$\begin{aligned}
\left(\int_{\mathcal{B}} p_i^{\text{lin.}}\mathrm{d}v\right)^{\cdot} &= \int_{\partial\mathcal{B}} \sigma_{ji}\mathrm{d}a_j + \int_{\mathcal{B}} \rho f_i \mathrm{d}v\,, \\
\left(\int_{\mathcal{B}} p_i^{\text{ang.}}\mathrm{d}v\right)^{\cdot} &= \int_{\partial\mathcal{B}} \alpha_{ji}\mathrm{d}a_j + \int_{\mathcal{B}} \rho z_i \mathrm{d}v\,,
\end{aligned} \tag{7}$$

where $p_i^{\text{lin.}}$, σ_{ij}, f_i are the linear momentum density (per volume), the flux of linear momentum, and the supply of linear momentum, respectively. $p_i^{\text{ang.}}$, α_{ij}, z_i denote the angular momentum density, the flux of angular momentum, and the supply term of angular momentum, respectively. The linear momentum density, $p_i^{\text{lin.}}$, and the angular momentum density, $p_i^{\text{ang.}}$, are conserved quantities, i.e., they are given in balance equations without production terms. They can be rewritten by using the specific (per mass) linear momentum and the specific angular momentum:

$$p_i^{\text{lin.}} = \rho v_i\,, \quad p_i^{\text{ang.}} = \rho a_i\,. \tag{8}$$

Moreover, the specific angular momentum is decomposed into an intrinsic specific spin, s_i, and into the moment of (specific linear) momentum:

$$a_i = s_i + \epsilon_{ijk} x_j v_k\,, \tag{9}$$

where we have introduced the LEVI-CIVITA symbol, ϵ_{ijk}. The flux of linear momentum, σ_{jk}, is the CAUCHY stress

tensor. Following (Müller (1973), Ch. II, § 2.d) we can multiply the balance of linear momentum in its local form by $\epsilon_{ijk}x_j$ and subtract the result from the balance of angular momentum for acquiring a balance of spin. The production term of the spin reads $\epsilon_{ijk}\sigma_{jk}$. For non-polar media the spin and its production vanish, i.e., $s_i = 0$ and $\epsilon_{ijk}\sigma_{jk} = 0$. This assumption leads to a symmetric CAUCHY stress tensor, $\sigma_{ij} = \sigma_{ji}$. A non-polar medium has no intrinsic spin such that the continuum possesses three degrees of freedom given by the displacement, u_i. For structures on the macroscale the balance of linear momentum is sufficient for calculating the displacement. The balance of angular momentum is automatically satisfied by a symmetric CAUCHY stress tensor, in other words, the flux of angular momentum is assumed to vanish. For structures on the microscale this assumption must be rediscussed and a model for the flux of angular momentum needs to be implemented.

The balance Eqs. 7 can be transformed onto the reference frame by using the solution for the balance of mass, $\rho_0 = \rho J$, with $J = \det(F_{ij})$. After applying GAUSS's theorem we obtain in every regular point of $\mathcal{B}_0$:

$$\begin{aligned}\rho_0\frac{\partial v_k}{\partial t} - \frac{\partial P_{rk}}{\partial X_r} - \rho_0 f_k = 0\,, \quad P_{rk} = (\boldsymbol{F}^{-1})_{rj}J\sigma_{jk}\,, \\ \rho_0\frac{\partial a_k}{\partial t} - \frac{\partial A_{rk}}{\partial X_r} - \rho_0 z_k = 0\,, \quad A_{rk} = (\boldsymbol{F}^{-1})_{rj}J\alpha_{jk}\,.\end{aligned} \tag{10}$$

Since the angular momentum consists of the spin and the moment of (linear) momentum, the flux of angular momentum, A_{ij}, can be decomposed into two parts where the first part is a flux of spin, μ_{ij}, and the second part is the moment of the flux of (linear) momentum:

$$A_{rk} = \mu_{rk} + \epsilon_{kji}X_jP_{ri}\,. \tag{11}$$

The flux of spin, μ_{ij}, is usually called a couple stress, as in (Mindlin and Tiersten 1962). Analogously, the supply of angular momentum reads

$$z_k = l_k + \epsilon_{kji}X_jf_i\,. \tag{12}$$

By following CAUCHY's tetrahedron argument, as in (Truesdell and Toupin (1960), Sect. 203), we relate the stress to a traction on the surface, t_i, and, analogously, the couple stress to a moment couple on the surface, m_i:

$$\sigma_{ij} = n_it_j\,, \quad \mu_{ij} = n_im_j\,. \tag{13}$$

Note that the moment couple m_j is an axial vector (pseudovector). Thus, it does not have the same transformation properties as a polar vector (tensor of rank one). Therefore, instead of the axial vectors, a_i, m_i, we use, as in (Truesdell and Toupin (1960), Sect. 203), the skew-symmetric form that is well-known in rigid body dynamics for the representation of the angular velocity. We change the balance of angular momentum in the reference frame into the skew-symmetric form:

$$\rho_0\frac{\partial a_{ik}}{\partial t} - \frac{\partial A_{irk}}{\partial X_r} - \rho_0 z_{ik} = 0\,, \tag{14}$$

with:

$$a_{ik} = \frac{1}{2}\epsilon_{ikj}a_j\,, \quad A_{irk} = \frac{1}{2}\epsilon_{ikj}A_{rj}\,, \quad z_{ik} = \frac{1}{2}\epsilon_{ikj}z_j\,. \tag{15}$$

Now by using the tensor identity:

$$\epsilon_{ikj}\epsilon_{jmn} = \epsilon_{jik}\epsilon_{jmn} = \delta_{im}\delta_{kn} - \delta_{in}\delta_{km}\,, \tag{16}$$

we obtain

$$\begin{aligned}A_{irk} &= \frac{1}{2}\epsilon_{ikj}\mu_{rj} + \frac{1}{2}\epsilon_{ikj}\epsilon_{jmn}X_mP_{rn} = \mu_{irk} \\ &\quad + \frac{1}{2}(X_iP_{rk} - X_kP_{ri}) = \mu_{irk} + X_{[i}P_{rk]}\,, \\ z_{ik} &= \frac{1}{2}\epsilon_{ikj}l_j + \frac{1}{2}\epsilon_{ikj}\epsilon_{jlm}X_lf_m = l_{ik} + \frac{1}{2}(X_if_k - X_kf_i) = l_{ik} + X_{[i}f_{k]}\,.\end{aligned} \tag{17}$$

Since we deal with a non-polar medium the specific angular momentum simplifies to

$$a_{ik} = \frac{1}{2}\epsilon_{ikj}a_j = \frac{1}{2}\epsilon_{ikj}\epsilon_{jlm}X_lv_m = \frac{1}{2}(X_iv_k - X_kv_i) = X_{[i}v_{k]}\,. \tag{18}$$

The skew-symmetric form was presented in a similar way in (Mindlin and Eshel 1968; Toupin 1962), (Truesdell and Toupin (1960), Sect. 205). However, the starting point and the motivation are different here.

The objective is to find such a displacement field, $u_i = x_i - X_i$, so that Eq. $(10)_1$ and Eq. (14) are satisfied. By using the time rate of displacements as the velocity:

$$v_i = \dot{x}_i = \dot{u}_i\,, \quad \text{since } \dot{X}_i = 0\,, \tag{19}$$

and by employing a comma for denoting the partial derivatives in X_i the balance equations of momenta read

$$\begin{aligned}\rho_0\ddot{u}_k - P_{rk,r} - \rho_0 f_k = 0\,, \\ \rho_0 X_{[i}\ddot{u}_{k]} - \mu_{irk,r} - P_{[ik]} - X_{[i}P_{rk],r} - \rho_0 l_{ik} - X_{[i}f_{k]} = 0\,.\end{aligned} \tag{20}$$

Since we will solve both of them simultaneously we can subtract the first one multiplied by $X_{[i}$ from the second one and obtain

$$\rho_0\ddot{u}_k - P_{rk,r} - \rho_0 f_k = 0\,, \quad -\mu_{irk,r} - P_{[ik]} - \rho_0 l_{ik} = 0\,. \tag{21}$$

These equations of motion include supply terms, f_i, l_{ij}, to be given and flux terms, P_{ij}, μ_{ijk}, to be defined with respect to the displacement (or its gradient). Only then Eqs. (21) are closed and can be solved.

Constitutive relations

In order to complete Eqs. (21) we need to define constitutive equations for the stress, P_{ij}, and for the couple stress,

μ_{ijk}. The main objective of the whole theory is to find the displacement, u_i. Therefore, the constitutive equations shall depend on $u_{i,j}$ and $u_{i,jk}$—this dependence is consistent with the motivation of the theory leading to Eqs. (6). Instead of $u_{i,j}$ we can employ the GREEN-LAGRANGE strain:

$$E_{ij} = \frac{1}{2}(C_{ij} - \delta_{ij}) \,, \quad C_{ij} = F_{ki}F_{kj} \,, \tag{22}$$

which is obviously symmetric. Instead of $u_{i,jk}$ we can apply the gradient of the GREEN-LAGRANGE strain, $E_{ij,k}$. Hence, the stress tensor and the couple stress tensor may depend on the strain and its gradient. We want to find out their general form for *linear* and *isotropic* materials. For a linear isotropic material the dependence of the stress on the strain gradient vanishes, as well as the couple stress fails to depend on the strain, see (dell'Isola et al. (2009), Sect. 3). Since the strain is a symmetric tensor, $E_{ij} = E_{ji}$, we use the second PIOLA-KIRCHHOFF stress tensor, $S_{kj} = (\boldsymbol{F}^{-1})_{ji}P_{ki}$, which is also symmetric, $S_{ij} = S_{ji}$, based on the definition of the first PIOLA-KIRCHHOFF stress tensor, P_{ij}, in Eq. $(10)_2$. Hence the general linear relations for the stress and the couple stress read

$$S_{ij} = C_{ijkl}E_{kl} \,, \quad \mu_{ijk} = D_{ijklmn}E_{lm,n} \,. \tag{23}$$

By following (Suiker and Chang 2000) we acquire the general tensorial form of isotropic tensors of rank four and six, i.e., for C_{ijkl} and D_{ijklmn}, respectively. For the sake of brevity we skip the detailed explanation that can be found in the Appendix starting on p. 9. An isotropic tensor of rank four from Eq. (68) on p. 10 reads

$$A_{ijkl} = c_1\delta_{ij}\delta_{kl} + c_2\delta_{ik}\delta_{jl} + c_3\delta_{il}\delta_{jk} \,. \tag{24}$$

We can use this form for C_{ijkl} and obtain the constitutive equation between S_{ij} and E_{ij} in Cartesian coordinates:

$$S_{ij} = C_{ijkl}E_{kl} \,, \quad C_{ijkl} = \lambda\delta_{ij}\delta_{kl} + \mu\delta_{ik}\delta_{jl} + \nu\delta_{il}\delta_{jk} \,. \tag{25}$$

Since $E_{ij} = E_{ji}$ we conclude that $\mu = \nu$ and obtain ST. VENANT's law for elasticity:

$$S_{ij} = \lambda E_{kk}\delta_{ij} + 2\mu E_{ij} \,, \tag{26}$$

where the LAMÉ parameters, λ, μ, are determined by using engineering constants, namely YOUNG's modulus, E, and POISSON's ratio, ν:

$$\lambda = \frac{E\nu}{(1+\nu)(1-2\nu)} \,, \quad \mu = \frac{E}{2(1+\nu)} \,. \tag{27}$$

Next we find D_{ijklmn} for isotropic materials by using the same procedure. We apply the relation in Eq. (70) on p. 15 for D_{ijklmn} in Eq. $(23)_2$, and obtain

$$\begin{aligned}\mu_{ijk} = {} & c_{01}\delta_{ij}E_{km,m} + c_{02}\delta_{ij}E_{lk,l} + c_{03}\delta_{ij}E_{ll,k} + c_{04}\delta_{ik}E_{jm,m} + \\ & + c_{05}\delta_{ik}E_{lj,l} + c_{06}\delta_{ik}E_{ll,j} + c_{07}\delta_{jk}E_{im,m} + c_{08}E_{ij,k} + \\ & + c_{09}E_{ik,j} + c_{10}\delta_{jk}E_{li,l} + c_{11}E_{ji,k} + c_{12}E_{ki,j} + \\ & + c_{13}\delta_{jk}E_{ll,i} + c_{14}E_{jk,i} + c_{15}E_{kj,i} \,.\end{aligned} \tag{28}$$

Fifteen parameters, $c_{01} \ldots c_{15}$, need to be determined. Since $E_{lm,n} = E_{ml,n}$ we obtain

$$\begin{aligned}\mu_{ijk} = {} & (c_{01} + c_{02})\delta_{ij}E_{km,m} + c_{03}\delta_{ij}E_{ll,k} + (c_{04} + c_{05})\delta_{ik}E_{jm,m} + \\ & + c_{06}\delta_{ik}E_{ll,j} + (c_{07} + c_{10})\delta_{jk}E_{im,m} + (c_{08} + c_{11})E_{ij,k} + \\ & + (c_{09} + c_{12})E_{ik,j} + c_{13}\delta_{jk}E_{ll,i} + (c_{14} + c_{15})E_{jk,i} \,.\end{aligned} \tag{29}$$

Hence the most general form of the couple stress or the flux of spin for linear elasticity has nine phenomenological constants. Quite often two more assumptions are made. First, one takes $\mu_{ijk} \approx \mu_{jik}$ for granted. Second, one assumes that $\mu_{ijk}E_{ij,k}$ is a part of the (deformation) energy, such that $D_{ijklmn} = D_{lmnijk}$ holds. Under these assumptions nine constants reduce to five material constants, see (dell'Isola et al. (2009), Eqs. (3.1)–(3.7)) and for an overview of such theories refer to (Askes and Aifantis (2011), Sect. 2). We try to avoid introducing assumptions restraining the formulation to specific type of materials.

In the last section we have obtained the governing equations. There have been some assumptions, which bring in further restrictions in order to make the form of D_{ijklmn} admissible with Eqs. (21). We can neglect the supply term l_{ik} or at least restrict it to be antisymmetric, $l_{ik} = -l_{ki}$. Hence we observe by inspecting Eq. $(21)_2$ that μ_{ijk} has to be antisymmetric in the indices i, k , i.e., $\mu_{ijk} = -\mu_{kji}$ or equivalently $\mu_{ijk} + \mu_{kji} = 0$. This condition implies

$$\begin{aligned}& c_{01} + c_{02} = -(c_{07} + c_{10}) \,, \quad c_{03} = -c_{13} \,, \\ & c_{04} + c_{05} = c_{06} = c_{09} + c_{12} = 0, \quad c_{08} + c_{11} = -(c_{14} + c_{15}) \,.\end{aligned} \tag{30}$$

After employing these restrictions and renaming the constants the couple stress reads

$$\begin{aligned}\mu_{ijk} = {} & \alpha\left(\delta_{ij}E_{km,m} - \delta_{jk}E_{im,m}\right) + \beta\left(\delta_{ij}E_{mm,k} - \delta_{jk}E_{mm,i}\right) + \\ & + \gamma\left(E_{ij,k} - E_{jk,i}\right) \,.\end{aligned} \tag{31}$$

In a heterogeneous material the material parameters, α, β, γ, can depend on position and they may also depend on temperature. Here we will implement them as constants

and investigate their roles in deformation. The constitutive Eq. (31) for the couple stress tensor and Eq. (26) for the stress tensor will be implemented in the numerical investigation.

There is a well-known material equation for the couple stress with one parameter, see for example (Gao and Park 2007):

$$\mu_{ijk} = cS_{jk,i}\,, \tag{32}$$

which is actually a special choice of the parameters of Eq. (31), α, β, and γ. In order to see this we insert Eq. (31) and Eq. (26) into Eq. (32) as follows

$$\begin{aligned}\alpha\left(\delta_{ij}E_{km,m}-\delta_{jk}E_{im,m}\right)+\beta\left(\delta_{ij}E_{mm,k}-\delta_{jk}E_{mm,i}\right)+\\ +\gamma\left(E_{ij,k}-E_{jk,i}\right)=c\lambda E_{ll,i}\delta_{jk}+2c\mu E_{jk,i}\,.\end{aligned} \tag{33}$$

One possible choice of α, β, γ can be obtained by multiplying Eq. (33) with δ_{ij} and by using a direct analysis with the assumption of $\alpha=\beta$ such that:

$$\begin{aligned}&2\alpha E_{km,m}+2\beta E_{mm,k}+\gamma E_{ii,k}-\gamma E_{ik,i}=c\lambda E_{mm,k}+2c\mu E_{ik,i}\,,\\ &2\alpha-\gamma=2c\mu\,,\quad 2\beta+\gamma=c\lambda\,,\\ &\text{if}:\alpha=\beta\quad\Rightarrow\quad\alpha=\beta=c\left(\frac{\lambda}{4}+\frac{\mu}{2}\right)\,,\quad\gamma=c\left(\frac{\lambda}{2}-\mu\right)\,.\end{aligned} \tag{34}$$

Another possible choice results analogously by multiplying Eq. (33) with δ_{jk} and, again, by assuming $\alpha=\beta$ as follows

$$\begin{aligned}&-2\alpha E_{im,m}-2\beta E_{mm,i}+\gamma E_{ik,k}-\gamma E_{kk,i}=3c\lambda E_{ll,i}+2c\mu E_{kk,i}\,,\\ &-2\alpha+\lambda=0\,,\quad-2\beta-\lambda=3c\lambda+2c\mu\,,\\ &\text{if}:\alpha=\beta\quad\Rightarrow\quad\alpha=\beta=-c\left(\frac{3}{4}\lambda+\frac{\mu}{2}\right)\,,\quad\gamma=-c\left(\frac{3}{2}\lambda+\mu\right).\end{aligned} \tag{35}$$

Therefore, the constitutive Eq. (32) is a special choice of the proposed relation in Eq. (31). Of course the assumption $\alpha=\beta$ is difficult to justify. Thus we will use the more general formulation given by Eq. (31).

In the following section we will implement the balance Eqs. (21) complemented by the constitutive equations:

$$\begin{aligned}S_{ij}=\lambda E_{kk}\delta_{ij}+2\mu E_{ij}\,,\mu_{ijk}=\alpha\left(\delta_{ij}E_{km,m}-\delta_{jk}E_{im,m}\right)+\\ +\beta\left(\delta_{ij}E_{mm,k}-\delta_{jk}E_{mm,i}\right)+\gamma\left(E_{ij,k}-E_{jk,i}\right)\end{aligned} \tag{36}$$

in a numerical computational environment that allows us to comprehend the role of the parameters α, β, γ.

Computational approach

There are various numerical implementations of theories dealing with higher order materials. We skip a discussion of pros and cons between different implementations and refer to (Askes and Aifantis (2011), Sect. 5) instead. In this work we solve the balance equations complemented by the constitutive equations numerically in a discrete fashion, viz., by using the finite element method in space and the finite difference method in time. First, we obtain the so-called *weak* form for Eqs. (21) within a finite domain, Ω, in a standard manner by multiplying them with corresponding test functions and by performing integration by parts on the flux terms:

$$\begin{aligned}\mathrm{F}_1&=\int_\Omega\left(\rho_0\ddot{u}_k\delta u_k+P_{rk}\delta u_{k,r}-\rho_0 f_k\delta u_k\right)\mathrm{d}V-\int_{\partial\Omega}P_{rk}\delta u_k N_r\mathrm{d}A\,,\\ \mathrm{F}_2&=\int_\Omega\left(\mu_{irk}\delta u_{k,ir}-P_{[ik]}\delta u_{k,i}-\rho_0 l_{ik}\delta u_{k,i}\delta u_{k,i}\right)\mathrm{d}v-\int_{\partial\Omega}\mu_{irk}\delta u_{k,i}N_r\mathrm{d}A\,.\end{aligned} \tag{37}$$

The choice of the test functions can also be based on introducing a new field such as a rotation instead of $\delta u_{k,i}$, see for example (Bauer et al. 2012). However, because we want to determine the displacement field there is no reason or computational benefit to introduce another quantity such as a rotation field. Therefore, we use $\delta u_{k,i}$ and obtain two integrands in Eqs. (37) in the same unit of energy density. Hence we can sum them up:

$$\mathrm{F}=\mathrm{F}_1+\mathrm{F}_2\,. \tag{38}$$

The weak form, F, is of second-order in space regarding the displacement field. Therefore, we choose finite elements of the continuous GALERKIN type of second polynomial degree. In other words, the displacements and also their test functions are from a HILBERT space, $u_i,\delta u_i\in H^2$ as described in (Hilbert 1902). Moreover, their gradients have to exist, i.e., more specifically the solution space is a SOBOLEV space within the finite domain, referred to as *finite elements*. Elements are discrete subdomains, $\Omega^i\cap\Omega^j=\{\}\,,\forall i\neq j$, which collectively constitute the region, $\sum\Omega^e=\mathcal{B}_0$, where the computation takes place.

For the time discretization we use the *finite difference* method:

$$\frac{\partial(\cdot)}{\partial t}=\frac{(\cdot)-(\cdot)^0}{\Delta t}\,,\quad\Delta t=t^{(k+1)}-t^{(k)}\,, \tag{39}$$

where time is discretized as a list of length n equally separated, $t^{(k)}=\{\Delta t,2\Delta t,\dots\,n\Delta t\}$. This approach is simple and stable for real-valued problems because it is an *implicit* method. In order to see this, we can apply a TAYLOR expansion to the value (in any position) at the time instant $t^{(k)}$ in order to find the value (in the same position) at the time instant $t^{(k+1)}$ as follows

$$\begin{aligned}u_i\left(x_i,t^{(k)}\right)=u_i\left(x_i,t^{(k)}+\Delta t-\Delta t\right)=u_i\left(x_i,t^{(k+1)}-\Delta t\right)=\\ =u_i\left(x_i,t^{(k+1)}\right)-\Delta t\frac{\partial u_i}{\partial t}\left(x_i,t^{(k+1)}\right)\,,\end{aligned} \tag{40}$$

where the higher order terms are omitted subject to the condition that Δt is sufficiently small. Since the time derivative is evaluated at time $t^{(k+1)}$, for which the value

is sought, it is an implicit method. Obviously by rewriting the latter we acquire Eq. (39) for the time discretization. We employ the GALERKIN type *finite element* method, so that the test functions are chosen from the same SOBOLEV space as the displacements. Hence, the notation, δu_i, gets a fully consistent meaning. The weak form discretized in time and space by integrating over each finite element, Ω^e, and assembling by summing them up reads

$$\mathrm{F} = \sum_{\text{elements}} \int_{\Omega^e} \left(\rho_0 \frac{u_i - 2u_i^0 + u_i^{00}}{\Delta t \Delta t} \delta u_i + P_{ji} \delta u_{i,j} - \rho_0 f_i \delta u_i + \mu_{ijk} \delta u_{k,ij} - \right. \\ \left. - P_{[ik]} \delta u_{k,i} - \rho_0 l_{ik} \delta u_{k,i} \right) \mathrm{d}V - \int_{\partial\Omega} \left(P_{jk} \delta u_k + \mu_{ijk} \delta u_{k,i} \right) N_j \mathrm{d}A \,. \tag{41}$$

Since the latter functional or weak form is nonlinear in u_i we can only solve it by using a linearization. We use a NEWTON-RAPHSON linearization scheme at the level of differential equations. In other words, this linearization is implemented before the assembly operation (building matrices). Therefore, the success of the linearization depends only on the starting value for approximation. Since we solve the problem transiently the starting value is either the initial condition, which is exact, or the solution from the last time step, which is exact up to machine precision. The NEWTON-RAPHSON linearization can be realized as an expansion of the functional, $\mathrm{F} = \mathrm{F}(u_i, \delta u_j)$, for finding the values in the next time step, $u_i(t + \Delta t)$. For a sufficiently small Δt this can be rewritten into:

$$u_i(t + \Delta t) = u_i(t) + \Delta u_i(t) \,. \tag{42}$$

If the change, Δu_i, is small then the above relation yields the correct $u_i(t + \Delta t)$. If this is not the case, then we can solve it incrementally until $|\Delta u_i|$ is smaller than a given value (tolerance). For a small time step, Δt, this incremental approach leads to the correct solution. In order to find the increment, Δu_i, we can again employ a TAYLOR series truncated after linear terms on the functional:

$$\mathrm{F}(u_i + \Delta u_i, \delta u_i) = \mathrm{F}(u_i, \delta u_i) + J_i \, \Delta u_i \,, \tag{43}$$

where the JACOBIan, J_i, is simply the derivative of F with respect to the unknowns, u_i. Since the weak form shall be zero:

$$\mathrm{F}(u_i, \delta u_i) + J_i \, \Delta u_i = 0 \,, \tag{44}$$

we have obtained an equation linear in the increment, Δu_i, which is solvable. By updating the solution:

$$u_i := u_i + \Delta u_i \,, \tag{45}$$

and solving the increment once more until the value is smaller than the given tolerance, we determine the correct value of $u_i(t + \Delta t)$. We have programmed in Python and computed by using the novel collection of open-source packages, developed under FEniCS project (Logg et al. 2011). The *directional* derivative, $J_i \Delta u_i$, is calculated by using the following procedure:

$$J_i \, \Delta u_i = \frac{\mathrm{d}}{\mathrm{d}a} \mathrm{F}(u_i + a \Delta u_i, \delta u_i) \Big|_{a=0} \,. \tag{46}$$

This approach is fully automatized by using a symbolic derivation, see (Alnaes and Mardal 2010). Therefore, the only necessary input is the weak form given in Eq. (41). All 3D-visualizations are realized by using ParaView.[1] All 2D-plots were created by MatpPlotLib packages, see (Hunter 2007), developed for NumPy, see (Oliphant 2007). The code used for solving the examples in the next section is published in (Abali 2015) under GNU public license as declared in (Gnu Public 2007).

Results

In order to analyze the effect of the material parameters, α, β, γ in the proposed constitutive equation for the couple stress μ_{ijk} we construct a simple example to solve. Consider a three-dimensional beam clamped on one end which deforms when subjecting it to a shear loading on the other end. The beam is of length 10 μm. It is a slender beam since its width/length and height/length ratios are both 1/30. For all calculations we use the material parameters of generic aluminum:

$$\rho = 2700 \cdot 10^{-15} \, \mathrm{g/\mu m^3} \,, \quad E = 72 \, \mathrm{GPa} \hat{=} \mathrm{mN/\mu m^2} \,, \quad \nu = 0.33 \,. \tag{47}$$

We analyze three different loadings, viz., shear loading, tensile loading, and torsion. The loading has been implemented as a NEUMANN boundary condition at the end of the beam in Eq. (41) by defining a traction vector, $\hat{t}_i$, as follows

$$\hat{t}_k = P_{jk} N_j \tag{48}$$

Since the other boundaries are free the traction vanishes. Analogously a traction for the couple stress can be defined

$$\hat{\tau}_{ki} = \mu_{ijk} N_j \tag{49}$$

causing a spin on the boundaries by applying a moment at the micron scale. For free boundaries as well as for the both ends we assume that the system is lacking such a traction. We employ homogeneous NEUMANN, in other words, *natural* boundary conditions for the couple stress term. For each one of the loadings we have performed four simulations:

$$\begin{aligned} \text{Sim. I (color: gray)} &: \alpha = 0 \, \mathrm{mN} \,, \quad \beta = 0 \, \mathrm{mN} \,, \quad \gamma = 0 \, \mathrm{mN} \,, \\ \text{Sim. II (color: red)} &: \alpha = -1 \, \mathrm{mN} \,, \quad \beta = 0 \, \mathrm{mN} \,, \quad \gamma = 0 \, \mathrm{mN} \,, \\ \text{Sim. III (color: green)} &: \alpha = 0 \, \mathrm{mN} \,, \quad \beta = -1 \, \mathrm{mN} \,, \quad \gamma = 0 \, \mathrm{mN} \,, \\ \text{Sim. IV (color: blue)} &: \alpha = 0 \, \mathrm{mN} \,, \quad \beta = 0 \, \mathrm{mN} \,, \quad \gamma = -1 \, \mathrm{mN} \,. \end{aligned} \tag{50}$$

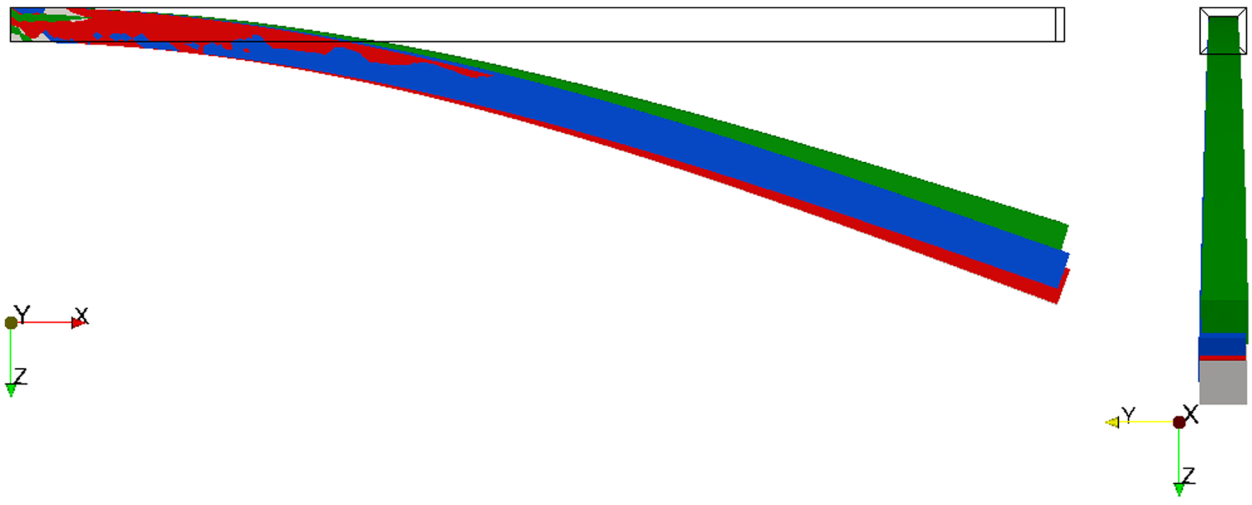

Fig. 1 Shear loading. The initial shape of the beam is outlined by black lines. Gray (Sim. I), red (Sim. II), green (Sim. III), blue (Sim. IV) beams present the 50 times upscaled deformed shape with different material parameters

For each loading case we present all simulations and by comparing them we try to comprehend the effects of the α, β, γ parameters on the deformation. We start with shear loading. The beam lies along the x-axis and the loading at the tip is applied in z-direction. All simulations can be seen in Fig. 1.

The initial shape is denoted by black lines. The classical beam bending (without couple stress) is colored in gray for comparison. The parameter $\alpha = -1$ (red) has an insignificant effect relative to the parameters $\beta = -1$ (green) and $\gamma = -1$ (blue). The green and blue colored deformations present an additional bending, such that the amount of bending on yz-plane decreases. In other words, the beam responds stiffer to shear loading in case of existing β or γ parameters.

Next we analyze tensile loading. The same configuration for simulations has been used and the results are presented in Fig. 2 by using the same colors.

The initial geometry is again denoted by black lines, we have tilted the geometry for better visualization. The gray deformation is the classical stretching without couple stress. The effect of α (red) is significant again by causing an additional bending motion. Relative to the effect of α the effects of β and γ can be neglected.

Finally we analyze torsion. Four simulations with the previous color codings are depicted in Fig. 3.

The initial shape can be seen in black lines in the front view. In this case γ (blue) causes the most significant deviation from the classical solution (gray) without couple stress.

By observing the three loading cases we can conceive possibilities for measuring the parameters, α, β, γ. During shear loading the effects due to the α and γ parameters are smaller than the effect of β, such that it may be neglected. For tensile loading the effects of β and γ are smaller than α and may be ignored. In torsion the effect of α is significant and the effects of β and γ may be neglected. Under these simplifications the parameter α (red) can be measured by a tensile test by assuming that green and blue deformations are the same as the gray deformation in Fig. 2. The parameter β (green) can be measured by a shear test with the simplification that the red, blue, and

Fig. 2 Tensile loading. The initial shape of the beam is outlined by black lines. Gray (Sim. I), red (Sim. II), green (Sim. III), blue (Sim. IV) beams present the 50 times upscaled deformed shape with different material parameters

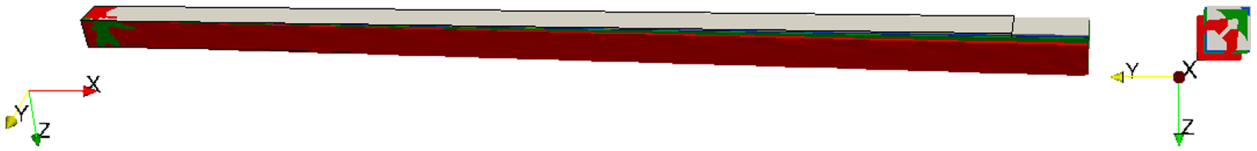

Fig. 3 Torsional loading. The initial shape of the beam is outlined by black lines. Gray (Sim. I), red (Sim. II), green (Sim. III), blue (Sim. IV) beams present the 50 times upscaled deformed shape with different material parameters

gray deformations are the same in Fig. 1. The parameter γ (blue) could be measured by a torsion test under the assumption that the red and green deformations in Fig. 3 are the same as the gray deformation.

The proposed strain gradient theory is an extension of the classical elasticity theory. Therefore, in the limit, strain gradient theory has to correspond to the classical theory of elasticity. In other words, the effect of couple stress should decrease while increasing the size of the geometry. We can examine the correspondence between strain gradient and classical elasticity by using an analytic solution. The EULER-BERNOULLI beam theory presents a closed-form solution for a *slender* beam in elastostatics. If the geometry is such that the length, ℓ, is ten times more than its width and thickness, then the beam can be considered as being slender. The deflection, w, of such a beam is well known as a function along the axis:

$$w = \frac{F\ell^3}{6EI}\left(3\left(\frac{x}{\ell}\right)^2 - \left(\frac{x}{\ell}\right)^3\right), \tag{51}$$

where the load, F, is the bending force shearing at tip of the beam, $x = \ell$, and the modulus of elasticity E together with the moment of inertia I result in a bending rigidity EI along the axis of the deflection. We consider a rectangular cross sectional area with width and height, b, h, respectively. The bending is on the axis along the width so that the moment of inertia becomes

$$I = \frac{bh^3}{12}. \tag{52}$$

By inserting the moment of inertia, we obtain

$$E = \frac{4F}{bu_z^{\max.}}\left(\frac{\ell}{h}\right)^3, \tag{53}$$

if we consider the deflection at the end of the beam, $w(x = \ell) = u_z^{\max.}$. Since the modulus of elasticity shall be constant in classical beam theory we can compute $u_z^{\max.}$ by an appropriate simulation for a three-dimensional continuum body with varying beam's length ℓ (and holding the geometric ratio fixed, $\ell/h = 30$). According to classical beam theory the ratio of shearing force to deflection at the tip shall be constant in beam's length. However, experimental results demonstrate that a smaller beam presents a stiffer behavior, see (Lam et al. 2003) and McFarland and Colton (2005). We have observed this *stiffening* phenomenon in Fig. 1 for one specific length. Now we vary the length for the beam and examine the correspondence of strain gradient theory to classical elasticity by using the following parameters:

$$\rho = 2700 \cdot 10^{-15}\,\mathrm{g/\mu m^3}, \quad E = 72\,\mathrm{GPa\hat{a}=mN/\mu m^2}, \quad \nu = 0.33,$$
$$\alpha = 0\,\mathrm{mN}, \quad \beta = -1\,\mathrm{mN}, \quad \gamma = 0\,\mathrm{mN}. \tag{54}$$

The numerical results have been compiled in Table 1.

Due to the parameter β the size effect is significant and it is qualitatively consistent with the experimental results presented in (Lam et al. (2003), Fig. 12). In Fig. 4 we demonstrate this by simulating with $\beta = -1$ mN (with couple stress) and also with $\beta = 0$ mN (without couple stress) in order to verify that the code works as expected.

As discussed previously the stiffening behavior is due to additional bending resulting from the couple stress. However, this bending does not affect the curvature. We have observed this behavior by plotting the normalized (with respect to the tip deflection) z-displacement of each beam. Since the curvature remains the same, we omit to present the results.

We emphasize that the material constant, E, does not change in reality. This example demonstrates that the beam when treated as a continuous body by using strain gradient elasticity responds stiffer than predicted by the EULER-BERNOULLI beam theory.

Table 1 Variation of YOUNG's modulus predicted by the EULER-BERNOULLI beam theory for the ratio $\ell/h = \ell/b = 30$ in case of changing the length of the beam

ℓ in µm	$u_z^{\max}$ in µm	E in mN/µm^2 = GPa
100	$495.19 \cdot 10^{-3}$	73
60	$176.05 \cdot 10^{-3}$	74
20	$17.72 \cdot 10^{-3}$	81
10	$4.11 \cdot 10^{-3}$	88
5	$0.96 \cdot 10^{-3}$	94

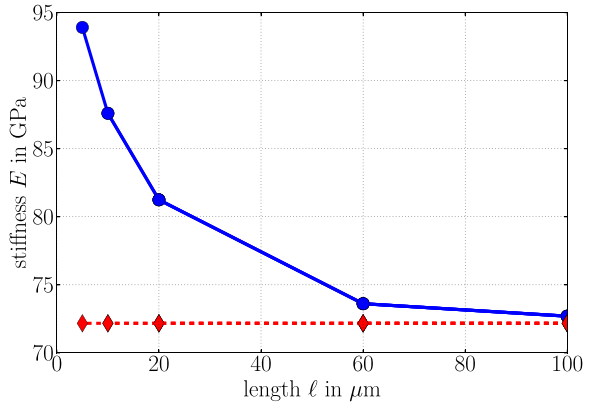

Fig. 4 Stiffening due to the size effect. The blue dots (connected with the continuous line) denote simulations with $\beta = -1$ mN and the red diamonds (connected with the dashed line) are computed by setting $\beta = 0$ mN. By increasing the length of beam, ℓ, the strain gradient corresponds with the classical theory

Conclusion

We have briefly outlined strain gradient elasticity from a continuum mechanics perspective. Starting from the balances of momenta we have obtained the so-called stress and couple stress tensors (of rank two and three, respectively). By applying general tensor relations we have obtained the necessary constitutive equations for the stress and for the couple stress. It is significant that we have proposed a couple stress with three material parameters, viz., α, β, and γ. In order to comprehend their impact during deformation we have implemented a numerical solution procedure where the discretization in time has been combined with the finite difference method. The discretization in space was realized with the finite element method. By simulating different loading cases we analyzed the couple stress parameters. We also verified the proposed theory qualitatively by establishing a simulation of the size effect.

There have been three main difficulties that we have overcome with some assumptions and left their discussions to further studies. The first difficulty arises by motivating a flux of spin in a non-polar medium. Since spin fails to exist in a non-polar medium and since we have assumed that the CAUCHY stress tensor is symmetric (so that the spin production vanishes), it is rather difficult to justify why the flux of angular momentum (couple stress) should exist. Nonetheless, our objective has been the modeling of couple stress for a non-polar medium. The second difficulty lies in determining a description for a measurement procedure for the material parameters in the proposed couple stress, namely α, β, γ. We have discussed their possible measurement after some assumptions, where α is determined by tensile, β by shear, and γ by torsion. However, the correctness of simplifications based on these assumptions is difficult to test. The third difficulty arises by varying the material parameters in order to comprehend their roles quantitatively. Their effects seem to be counter-intuitive and difficult to explain in a straightforward way. Numerical problems arise by choosing positive or greater values for the parameters. Unfortunately, we could not find general conditions in order to restrict the possible values of parameters. For using positive definiteness or thermodynamical laws we need to define the energy due to the spin. Spin is assumed to vanish and the stored energy is not uniquely defined for strain gradient theory. Therefore, the verification of the chosen parameters, and thus, the validation of presented results seem to be more difficult than expected. Any quantitative verifications by using experiments have been left to further research.

Endnote

[1]http://www.paraview.org

Appendix

A EUCLIDian transformation expressed in a Cartesian coordinate system:

$$x_{i'} = O_{i'j} x_j + b_{i'} \,, \quad O_{i'j} = O_{i'j}(t) \,, \quad b_{i'} = b_{i'}(t) \,, \quad \frac{\partial x_{i'}}{\partial x_j} = O_{i'j} \,, \tag{55}$$

results in an *objective* tensor being transformed as:

$$A_{i'j'k'\ldots r'} = O_{i'i} O_{j'j} O_{k'k} \ldots O_{r'r} A_{ijk\ldots r} \,, \tag{56}$$

where $O_{i'j}$ is a rotation tensor, $\boldsymbol{O}^{-1} = \boldsymbol{O}^T$ and $\det(\boldsymbol{O}) = 1$, between two Cartesian coordinate systems characterized by *orthonormal* base vectors. An arbitrary tensor, $\boldsymbol{B}$, is referred to as an *isotropic* tensor if its components in any *orthogonal* coordinate system transform such that:

$$\begin{aligned} B_{i'j'k'\ldots r'} &= Q_{i'i} Q_{j'j} Q_{k'k} \ldots Q_{r'r} B_{ijk\ldots r} \,, \\ B_{ijk\ldots r} &= B_{i'j'k'\ldots r'} Q_{i'i} Q_{j'j} Q_{k'k} \ldots Q_{r'r} \,, \end{aligned} \tag{57}$$

where Q_{ij} is a proper transformation between two arbitrary *orthogonal* coordinate systems. Therefore, an objective tensor is isotropic under rotations:

$$\begin{aligned} A_{i'j'k'\ldots r'} &= O_{i'i} O_{j'j} O_{k'k} \ldots O_{r'r} A_{ijk\ldots r} \,, \\ A_{ijk\ldots r} &= A_{i'j'k'\ldots r'} O_{i'i} O_{j'j} O_{k'k} \ldots Q_{r'r} \,. \end{aligned} \tag{58}$$

Every even or odd *formal orthogonal invariant polynomial* function depending on n vectors:

$$F = F\left(a_i^{(1)}, a_i^{(2)}, \ldots, a_i^{(n)}\right) \,, \tag{59}$$

can be represented in a linear form:

$$F = c_1 F_1 + c_2 F_2 + \cdots + c_m F_m \,, \tag{60}$$

where the scalar functions, F_1, F_2, …, F_m, are built by two different combinations of its arguments, $a_i^{(1)}, a_i^{(2)}, \ldots, a_i^{(n)}$. The first combination is the sum of scalar products of every set of two vectors:

$$\boldsymbol{a}^{(\alpha)} \cdot \boldsymbol{a}^{(\beta)} = \delta_{ij} a_i^{(\alpha)} a_j^{(\beta)} , \quad \alpha \neq \beta . \tag{61}$$

The second combination is to use the determinant for every set of l odd vectors:

$$\det\left(a_i^{(1)} a_j^{(2)} \ldots a_r^{(l)}\right) = \epsilon_{ij\ldots r} a_i^{(1)} a_j^{(2)} \ldots a_r^{(l)} . \tag{62}$$

In the Cartesian coordinate system the KRONECKER symbol, δij, is the metric tensor:

$$\delta_{ij} = \begin{cases} 1 \text{ if } i = j \\ 0 \text{ otherwise} \end{cases} , \tag{63}$$

and the LEVI-CIVITA symbol, $\epsilon_{ij\ldots r}$, is equal to the permutation symbol:

$$\epsilon_{ij\ldots r} = \begin{cases} +1 \text{ if } ij\ldots r \text{ is an even permutation of } 1, 2, \ldots m \\ -1 \text{ if } ij\ldots r \text{ is an odd permutation of } 1, 2, \ldots m \\ 0 \quad \text{otherwise} \end{cases} . \tag{64}$$

Both, δij and $\epsilon_{ij\ldots r}$, are isotropic tensors, therefore, the following relation holds for an isotropic tensor, $A_{ij\ldots r}$:

$$F\left(\boldsymbol{a}^{(1)}, \boldsymbol{a}^{(2)}, \ldots, \boldsymbol{a}^{(n)}\right) = A_{ij\ldots r} a_i^{(1)} a_j^{(2)} \ldots a_r^{(n)} . \tag{65}$$

Consider an isotropic tensor of rank two, A_{ij}. We apply the procedure:

$$\begin{aligned} A_{ij} a_i^{(1)} a_j^{(2)} &= F\left(\boldsymbol{a}^{(1)}, \boldsymbol{a}^{(2)}\right) = c_1 \delta_{ij} a_i^{(1)} a_j^{(2)} , \\ A_{ij} &= c_1 \delta_{ij} , \end{aligned} \tag{66}$$

since the arguments are arbitrary. The constant c_1 is called the material parameter in a constitutive equation relating two tensors of rank one.

Consider an isotropic tensor of rank three, A_{ijk}. In this case we obtain

$$\begin{aligned} A_{ijk} a_i^{(1)} a_j^{(2)} a_k^{(3)} &= F\left(\boldsymbol{a}^{(1)}, \boldsymbol{a}^{(2)}, \boldsymbol{a}^{(3)}\right) = c_1 \epsilon_{ijk} a_i^{(1)} a_j^{(2)} a_k^{(3)} , \\ A_{ijk} &= c_1 \epsilon_{ijk} , \end{aligned} \tag{67}$$

where c_1 is again a parameter to be determined for a constitutive equation relating a tensor of rank one to a tensor of rank two. For an isotropic tensor of rank four, A_{ijkl}, which is indeed necessary for Eq. $(23)_1$, we make use of the same approach and acquire

$$\begin{aligned} A_{ijkl} a_i^{(1)} a_j^{(2)} a_k^{(3)} a_l^{(4)} &= F\left(\boldsymbol{a}^{(1)}, \boldsymbol{a}^{(2)}, \boldsymbol{a}^{(3)}, \boldsymbol{a}^{(4)}\right) = c_1 \delta_{ij} a_i^{(1)} a_j^{(2)} \delta_{kl} a_k^{(3)} a_l^{(4)} + \\ &+ c_2 \delta_{ik} a_i^{(1)} a_k^{(3)} \delta_{jl} a_j^{(2)} a_l^{(4)} + c_3 \delta_{il} a_i^{(1)} a_l^{(4)} \delta_{jk} a_j^{(2)} a_k^{(3)} , \\ A_{ijkl} &= c_1 \delta_{ij} \delta_{kl} + c_2 \delta_{ik} \delta_{jl} + c_3 \delta_{il} \delta_{jk} . \end{aligned} \tag{68}$$

For the case of a tensor of rank six the methodology is similar:

$$\begin{aligned} A_{ijklmn} a_i^{(1)} a_j^{(2)} a_k^{(3)} a_l^{(4)} a_m^{(5)} a_n^{(6)} &= F\left(\boldsymbol{a}^{(1)}, \boldsymbol{a}^{(2)}, \boldsymbol{a}^{(3)}, \boldsymbol{a}^{(4)}, \boldsymbol{a}^{(5)}, \boldsymbol{a}^{(6)}\right) = \\ &= c_{01} \delta_{ij} a_i^{(1)} a_j^{(2)} \delta_{kl} a_k^{(3)} a_l^{(4)} \delta_{mn} a_m^{(5)} a_n^{(6)} + c_{02} \delta_{ij} a_i^{(1)} a_j^{(2)} \delta_{km} a_k^{(3)} a_m^{(5)} \delta_{ln} a_l^{(4)} a_n^{(6)} + \\ &+ c_{03} \delta_{ij} a_i^{(1)} a_j^{(2)} \delta_{kn} a_k^{(3)} a_n^{(6)} \delta_{ml} a_m^{(5)} a_l^{(4)} + c_{04} \delta_{ik} a_i^{(1)} a_k^{(3)} \delta_{jl} a_j^{(2)} a_l^{(4)} \delta_{mn} a_m^{(5)} a_n^{(6)} + \\ &+ c_{05} \delta_{ik} a_i^{(1)} a_k^{(3)} \delta_{jm} a_j^{(2)} a_m^{(5)} \delta_{ln} a_l^{(4)} a_n^{(6)} + c_{06} \delta_{ik} a_i^{(1)} a_k^{(3)} \delta_{jn} a_j^{(2)} a_n^{(6)} \delta_{lm} a_l^{(4)} a_m^{(5)} + \\ &+ c_{07} \delta_{il} a_i^{(1)} a_l^{(4)} \delta_{jk} a_j^{(2)} a_k^{(3)} \delta_{mn} a_m^{(5)} a_n^{(6)} + c_{08} \delta_{il} a_i^{(1)} a_l^{(4)} \delta_{jm} a_j^{(2)} a_m^{(5)} \delta_{kn} a_k^{(3)} a_n^{(6)} + \\ &+ c_{09} \delta_{il} a_i^{(1)} a_l^{(4)} \delta_{jn} a_j^{(2)} a_n^{(6)} \delta_{mk} a_m^{(5)} a_k^{(3)} + c_{10} \delta_{im} a_i^{(1)} a_m^{(5)} \delta_{jk} a_j^{(2)} a_k^{(3)} \delta_{ln} a_l^{(4)} a_n^{(6)} + \\ &+ c_{11} \delta_{im} a_i^{(1)} a_m^{(5)} \delta_{jl} a_j^{(2)} a_l^{(4)} \delta_{kn} a_k^{(3)} a_n^{(6)} + c_{12} \delta_{im} a_i^{(1)} a_m^{(5)} \delta_{jn} a_j^{(2)} a_n^{(6)} \delta_{lk} a_l^{(4)} a_k^{(3)} + \\ &+ c_{13} \delta_{in} a_i^{(1)} a_n^{(6)} \delta_{jk} a_j^{(2)} a_k^{(3)} \delta_{lm} a_l^{(4)} a_m^{(5)} + c_{14} \delta_{in} a_i^{(1)} a_n^{(6)} \delta_{jl} a_j^{(2)} a_l^{(4)} \delta_{km} a_k^{(3)} a_m^{(5)} + \\ &+ c_{15} \delta_{in} a_i^{(1)} a_n^{(6)} \delta_{jm} a_j^{(2)} a_m^{(5)} \delta_{kl} a_k^{(3)} a_l^{(4)} , \end{aligned} \tag{69}$$

thus we obtain

$$\begin{aligned} A_{ijklmn} = {} & c_{01} \delta_{ij} \delta_{kl} \delta_{mn} + c_{02} \delta_{ij} \delta_{km} \delta_{ln} + c_{03} \delta_{ij} \delta_{kn} \delta_{ml} + c_{04} \delta_{ik} \delta_{jl} \delta_{mn} + \\ & + c_{05} \delta_{ik} \delta_{jm} \delta_{ln} + c_{06} \delta_{ik} \delta_{jn} \delta_{lm} + c_{07} \delta_{il} \delta_{jk} \delta_{mn} + c_{08} \delta_{il} \delta_{jm} \delta_{kn} + \\ & + c_{09} \delta_{il} \delta_{jn} \delta_{mk} + c_{10} \delta_{im} \delta_{jk} \delta_{ln} + c_{11} \delta_{im} \delta_{jl} \delta_{kn} + c_{12} \delta_{im} \delta_{jn} \delta_{lk} + \\ & + c_{13} \delta_{in} \delta_{jk} \delta_{lm} + c_{14} \delta_{in} \delta_{jl} \delta_{km} + c_{15} \delta_{in} \delta_{jm} \delta_{kl} . \end{aligned} \tag{70}$$

Competing interests
The authors declare that they have no competing interests.

Authors' contributions
B.E.A. developed the theory, derived the weak form, and carried out the numerical computations. W.H.M. and V.A.E. discussed the theory and results, commented on the manuscript.

Author details
[1]Technische Universität Berlin, Institute of Mechanics, Einsteinufer 5, D10587 Berlin, Germany. [2]Otto-von-Guericke-Universität, Institute of Mechanics, Universitätsplatz 2, D39106 Magdeburg, Germany.

Received: 10 February 2015 Accepted: 5 June 2015
Published online: 08 July 2015

References

Abali BE (2015) Technical University of Berlin, Institute of Mechanics, Chair of Continuums Mechanics and Material Theory, Computational Reality. http://www.lkm.tu-berlin.de/ComputationalReality/, accessed 24 June 2015

Alnaes MS, Mardal KA (2010) On the efficiency of symbolic computations combined with code generation for finite element methods. ACM Trans Math Softw 37(1):6–1626

Askes H, Aifantis EC (2011) Gradient elasticity in statics and dynamics: An overview of formulations, length scale identification procedures, finite element implementations and new results. Int J Solids Struct 48(13):1962–1990

Bauer S, Dettmer W, Peric D, Schäfer M (2012) Micropolar hyperelasticity: constitutive model, consistent linearization and simulation of 3d scale effects. Comput Mech 50(4):383–396

dell'Isola F, Sciarra G, Vidoli S (2009) Generalized Hooke's law for isotropic second gradient materials. Proc R Soc A: Math Phys Eng Sci 465:2177–2196

Gao XL, Park SK (2007) Variational formulation of a simplified strain gradient elasticity theory and its application to a pressurized thick-walled cylinder problem. Int J Solids Struct 44(22-23):7486–7499. doi:10.1016/j.ijsolstr.2007.04.022

Gnu Public (2007) GNU General Public License. http://www.gnu.org/copyleft/gpl.html, accessed 24 June 2015

Gurtin ME, Fried E, Anand L (2010) The Mechanics and Thermodynamics of Continua. Cambridge University Press, Cambridge, UK

Hilbert D (1902) (transl. by E. J. Townsend), The foundations of geometry. The Open Court Publishing Co, Chicago
Hunter JD (2007) Matplotlib: A 2d graphics environment. Comput Sci Eng 9(3):90–95
Jones E, Oliphant T, Peterson P, et al (2001) SciPy: Open source scientific tools for Python. http://www.scipy.org/, accessed 24 June 2015
Logg A, Mardal KA, Wells GN (2011) Automated Solution of Differential Equations by the Finite Element Method, the FEniCS book. Lecture Notes in Computational Science and Engineering, Vol. 84. Springer, Berlin, Heidelberg
Lam D, Yang F, Chong A, Wang J, Tong P (2003) Experiments and theory in strain gradient elasticity. J Mech Phys Solids 51(8):1477–1508
McFarland AW, Colton JS (2005) Role of material microstructure in plate stiffness with relevance to microcantilever sensors. J Micromech Microeng 15(5):1060–1067
Mindlin RD, Tiersten HF (1962) Effects of couple-stresses in linear elasticity. Arch Ration Mech Anal 11:415–448. 10.1007/BF00253946
Mindlin RD, Eshel NN (1968) On first strain-gradient theories in linear elasticity. Int J Solids Struct 4(1):109–124
Morrison J (1939) The yield of mild steel with particular reference to the effect of size of specimen. Proc Inst Mech Eng 142(1):193–223
Müller I (1973) Thermodynamik. Bertelsmann-Universitätsverlag, Düsseldorf
Oliphant TE (2007) Python for scientific computing. Comput Sci Eng 9(3):10–20
Suiker A, Chang C (2000) Application of higher-order tensor theory for formulating enhanced continuum models. Acta Mechanica 142(1-4):223–234
Toupin RA (1962) Elastic materials with couple-stresses. Arch Ration Mech Anal 11:385–414
Truesdell C, Toupin RA (1960) The classical field theories. In: Flügge S (ed). Encyclopedia of physics, volume III/1, principles of classical mechanics and field theory. Springer, Berlin, Göttingen, Heidelberg. pp 226–790